Study on Micro-Structure Rebuild Of Clay In Process Of Consolidation

GJRE Classification (FOR)
GJRE: E, 090503

Li Shun-qun[1], Ling-xia Gao[2], CHAI Shou-xi[3]

***Abstract*-Vacuum freeze drying method is applied to prepare samples for SEM from one-dimensional consolidation clay which respectively suffered 5 grade pressures from original remolded state. And then simple and synthetical micro-structure parameters of SEM photos obtained from horizontal, 45° inclined and vertical section are studied to uncover relation between macroscopical mechanics properties and micro-structure. Study on simple parameters indicated that grain area ratio and perimeter increase with consolidation pressure while other parameters have no constant tendency. The synthetical parameters are derived from the two data analysis methods, namely principal component analysis and pedigree cluster. It is clearly shown that the first principal component approximately linear increases with consolidation pressure. Samples can be exactly clustered into several families according to the grade of consolidation pressure and inner distance of a family nonlinearly increases with pressure. It is distinct that the synthetical parameters are superior to the simple parameters in construction soil mechanics relation because the former can reflect the whole micro-structure qualities, but the latter cannot.**

Keywords- clay; one-dimensional consolidation; micro-structure rebuild; principal component analysis

I. Introduction

It is clear that characteristics and state of any material are determined by its corresponding micro-structure. For these materials like rock and soil, their properties of micro-structure can reflect not only their stress history, physical nature and mechanics feature, but their current status (Hu et al. 2001). At present, study on clay micro-structure and its relationship with macro-parameters becomes much hotter than ever and many methods or means have been introduced into the research field. As a result, some important conclusions were obtained by different researchers all over the world. For example, Tippkötter (2009) provided a method to detect soil water in macropores with X-ray tube computerized tomography utilized. And Kawaragi (2009) studied microstructure of saturated bentonites with X-ray CT technique employed.

In recent years, many researches worked hardly in order to bridge between micro-structure and macro-mechanics for different types of soil. Schäffer (2008, 2008) surveyed deformation and stability of macro-pore under uniaxial compression conditions. Chertkov (2008) thought that the intra-aggregate structure of a soil has important effect on its shrinkage characteristics. Agus (2005) studied the influence of shrinking and swelling on microstructures of a compacted bentonite-sand mixture.Bai (1997) peered the change of kaolin micro-structure in CD test. In confined condition, Cui (2002) studied micro-structure change of a swelling soil. With microstructure approach operated, Delage (2006) explored the ageing effects on a bentonite. After some experiments, Djéran-Maigre (1998) and Dudoignon (2001) bent themselves to constructed relationship between micro-structure and macroscopic properties respectively for clay and kaolinitic. Through investigation on micro-structure of Osaka Bay clay, Tanaka (1999) considered microfossils has impact on its mechanical behavior.

The Scan Electron microscope Method (SEM), together with various image processing techniques, can be utilized effectively to learn much about clay micro-structure. The SEM photos can show us much information about size, shape and distribution characters of pores and particles. Therefore, it is a good idea to bridge relationship between micro-structure and macromechanics for clay. In the process of information extraction, much more micro-parameters are picked up in order to acquire message as abundant as possible. Too much parameters, in one hand, can give us more information about characterizes of clay micro-structure, and in the other hand, result in message superposition and that make it difficult to apply micro-structure theory in soil mechanics. As a result, current study on relationship between micro-structure and macro-mechanics only can be conducted between certain single micro-structure parameter and certain macro-mechanics parameter. Therefore, it is necessary to bridge relationship between all-around micro-structure attributes and mechanics parameter.

Correlation analysis, principal component analysis and pedigree cluster analysis are the effective methods to study the extracted information, which can reduce dimension and evaluate characteristic from the original micro-structure parameters. The corresponding function of the methods is to build lower dimensional combined parameter from the higher dimensional parameters in which pertinence is prominent. Therefore, it is possible and reasonable to substitute simple parameters for complex parameters in the overall meanings while less information lost.

With the image manipulation software of Leica QWin utilized, the micro-structure parameters on different sections of samples, which were consolidated under five level pressures, are picked up firstly. And then, the lower dimensional synthetical parameters, including principal component index and interior (exterior) cluster distance, are

About-[1]. Department of Civil Engineering, Tianjin Institute of Urban Construction, Tianjin 300384
About[2].. Tianjin Key Laboratory of Soft Soil Characteristics and Engineering Environment, Tianjin 300384
About[3]- School of Architecture and Civil Engineering, Dalian nationalities University , Dalian 116600

constructed. After these, quantify and evaluation about different samples can be done with the synthetical parameters applied. It is concluded that the lower dimensional synthetical parameters can be used to substitute the original higher dimensional parameters with the reduplicate information filtrated. And the method can be used to describe the rebuild process of micro-structure simply and directly for clay consolidation.

II. BASIC PROPERTIES OF THE CLAY AND ITS CONSOLIDATION TEST

The studied clay was taken from a 35m depth bore drilled in the Key Project of Tianjin Railway Station. The main mechanics indexes of the clay constitute of the following: natural water content w=33%, void ratio e=0.735, natural gravity γ=19.8kN/m^3, internal friction angle φ=29.8^o, cohesion c=21.7kPa, compression index α_{1-2}=0.351MPa^{-1}, liquid limit w_l=31.8% and plastic limit w_p=21.2%.
The remolded samples were employed in this paper because of the anisotropic distribution of particles in vertical and horizontal direction due to sedimentation process. The undisturbed clay was oven-dried under 115^o conditions. The dried clay was taken out of the oven after 24h and comminuted in a breaking machine in order to remove geometrical and physical anisotropy. Then a 0.25mm sieve was used to wipe off larger particles and organic substance.
The clay power was put on a plate for sprinkling until reach the natural water content, w=35%. It is unnecessary to stir or mix the clay in order to make the remolded samples isotropy before the later mechanics experiments. The wetted clay and the plate were enclosed together in a three-layered plastic bag. A week later, water and air contained in the clay would arrive the equilibrium condition due to capillary action and thermal force. The 25 remolded samples, which were made by pressing method, were classified into 5 identical groups. And consolidation process was list as table 1. The prepared samples were located in WGD-Ⅱ consolidation apparatuses and undergo a process of 12.4kPa precompression for three days. After these, the common consolidation procedure was applied on these samples.

Group	The first	The second	The third	The fourth	The fifth
The load process /kPa	12.5	12.5	12.5	12.5	12.5
	25	25	25	25	25
	50	50	50	50	50
	100	100	100	100	100
		200	200	200	200
			400	400	400
				800	800
					1600

III. DEFINITION OF PARAMETERS FOR SEM PHOTOS

After the consolidation experiments completed, some specimens were made from the consolidated samples which were used to obtain micro-structure of the remolded samples. The specimens must be in the condition of high degree vacuum when observed by a scan electron microscope. Even micro-content pore water in existence in specimens, the obtained photos would be distorted ascribing to directly boil away of pore water. Therefore, some measure must be applied to ensure the specimens completely dry. The popular measures include natural drying, critical point drying and vacuum freeze drying and so on. The last method can't bring any damage to the specimens because of no any affection of pore water surface tension on particles. The direct freeze drying and the dewatering freeze drying are the main two freeze drying methods which were both employed in this paper.

The progress of direct freeze drying, including lower and higher vacuum degree phases, was conducted in the apparatus of vacuum freeze drying which can provide a vacuum of 10^{-4}Pa. After drying for about 13h, the dried specimens were taken out of the apparatus and sealed in a small plastic bag quickly in order to keep them far away from outer vapor.
The redundant electric charge will cumulate on the surface of specimen in the process of scanning because the dry clay is a nonconductor. This phenomenon will make the photo of clay micro-structure fuzzy due to charge and discharge ceaselessly. Therefore, it is important to make a conducting coat on the dried specimen before observed. The popular methods include metal coating, vacuum coating and getter coating. In this paper, the first method was applied to make the specimen conductible.

Then the specimens are fixed in the box of the scan electron microscope and the process of dewatering freeze drying is begun in order to lustrate vapor intruded into the specimens when coating. When the required vacuum condition in scan electron microscope is achieved, observation and photo taking can be commenced.
The concept of soil micro-structure lies in two aspects, which are particle micro-structure and pore micro-structure. Even the proposed method in this paper is aimed at the particle micro-structure, it has the same meaning with the pore micro-structure. In this study, the Leica QWin software was employed to pick up two types of micro-structure parameters, namely field micro-structure and feature micro-structure. The former, including the six original parameters and the six induced parameters, can provide information for the whole study domain. The later only can tell us information for one unit body. This study focuses on the most important parameters, the six field particle micro-structure parameters.
In order to obtain reasonable data, same analysis fields were chosen for every photo taken by the scan electron microscope as shown in Fig.1. The study domain is a square of 500 μm×500 μm. Here, p_i is the particle numbered i with horizontal intercept of ε_i and vertical intercept of v_i.

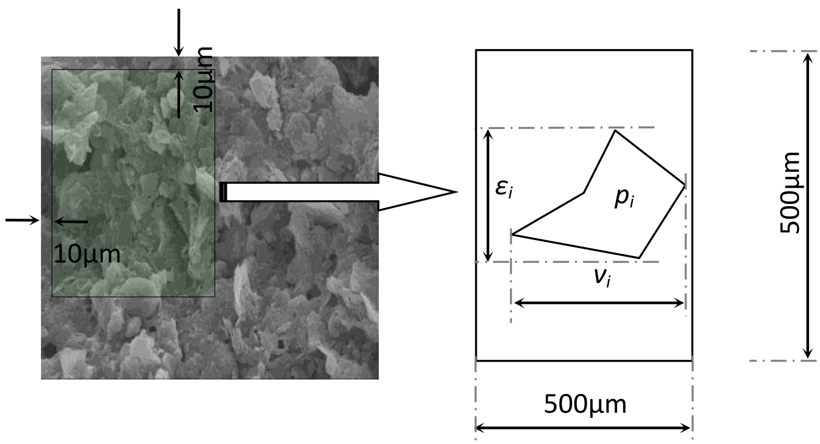

Fig. 1 Definition of particle micro-structure parameters

The obtained micro-structure parameters can be written as the followed matrix

$$x=\left(x_1,\ x_2,\ x_3,\ x_4,\ x_5,\ x_6\right)^{\mathrm{T}} \tag{1}$$

Here, x_1 and x_2 are respectively the sum of horizontal intercept of ε_i and the sum of vertical intercept of v_i, namely $x_1=\sum\varepsilon_i$ and $x_2=\sum v_i$. x_3 is the sum of the circumference of every particle in the domain, and x_5 is the arearatio of the total particle to field area. x_6 is a grey threshold determined by the Leica QWin software when the maximal variance of grey distribution achieved. It is clear that the primary properties of the particle micro-structure in the analysis field, including size, shape, gradation, anisotropy and so on, can be characterized by the stated parameters in formula (1).

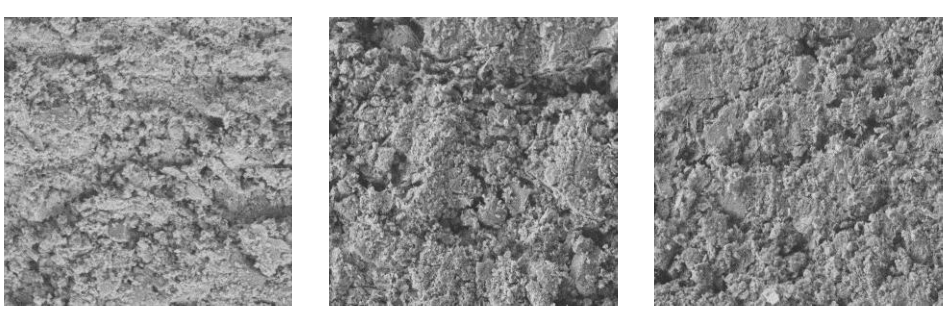

Section *A* Section *B* Section *C*

(a) 1600kPa

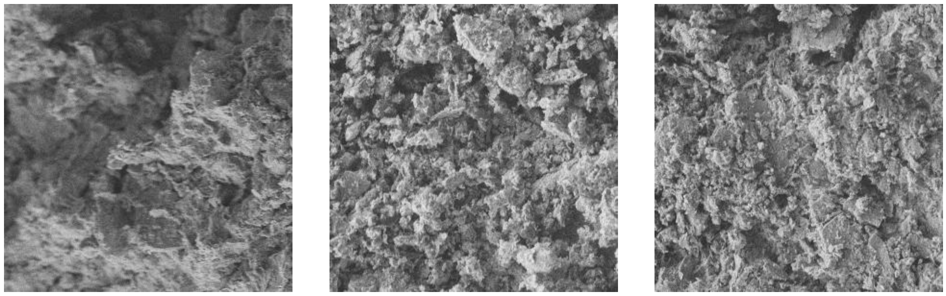

Section *A* Section *B* Section *C*

(b) 800kPa

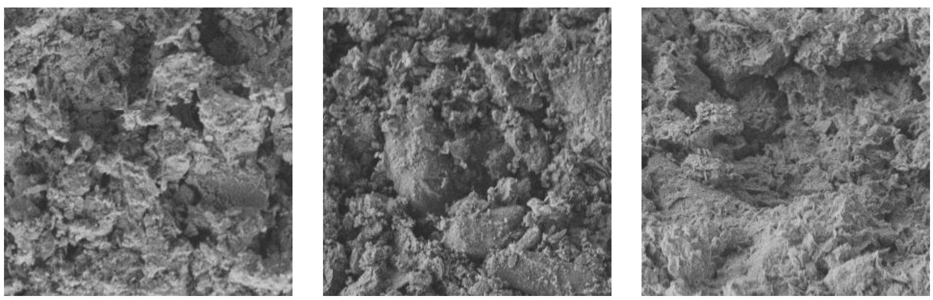

Section *A* Section *B* Section *C*

(c) 400kPa

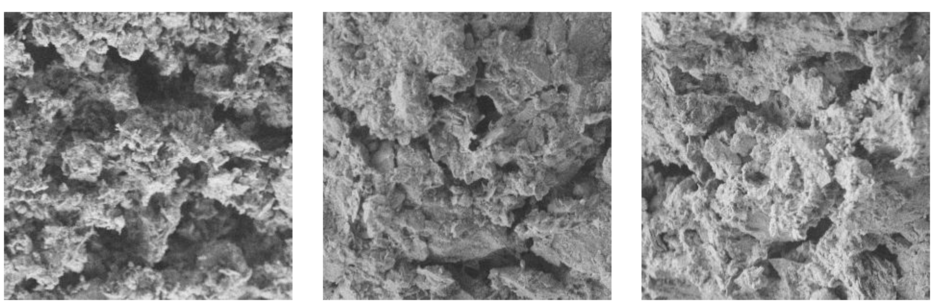

Section *A* Section *B* Section *C*

(d) 200kPa

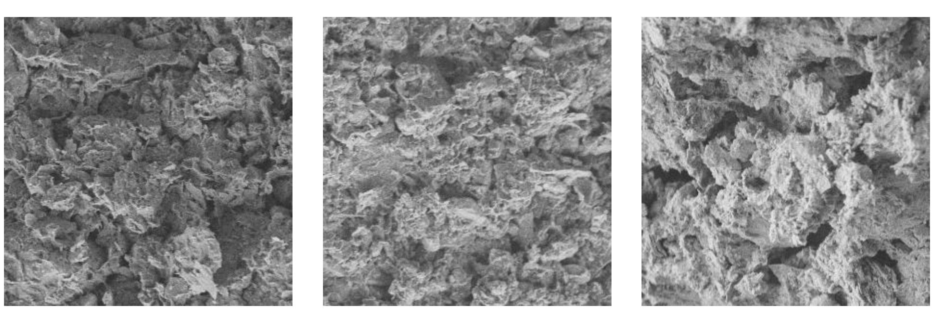

Section *A* Section *B* Section *C*

(e) 100kPa

Fig.2 SEM photos on the three planes from consolidated samples under the different pressure

The Fig.2 shows some SEM photos which were taken from different section of the samples. These sections are named as section *A*, section *B* and section *C* which are corresponding to vertical, 45^{o} inclined and horizontal direction. It can be seen that the total particle area in the analysis field increases with consolidation pressure for section *A*. Furthermore, same situation is for section *B* and section *C*.

In general, the particles micro-structure parameters in formula (1) picked-up directly from SEM photos can be called simple parameters because they only reflect one side of the photo. For example, x_3 can only give us information about circumference of particles, but not the shape. In fact, different parameter may give us some similar information about one character which is called overlapped information. For a certain type of soil, x_3 will rise with the increasing of x_5. The synthetical parameters are induced from the simple ones which can show us the overall meaning of the micro-structure. In addition, the synthetical parameter can remove the overlapped information displayed by the different simple parameter.

Owing to the points stated above, the construction of synthetical parameter and corresponding application in soil mechanics, especially for consolidation problem, will be studied carefully in the following part.

IV. PRINCIPAL COMPONENT ANALYSIS FOR MICRO-STRUCTURE

The method of principal component analysis aims at constructing a possible lower dimensional matrix from a higher dimensional matrix while the most information of the later is reserved. For example, the linear correlation relationship exists for a two-dimensional matrix, x=(x_1, x_2). An observed sample for the matrix is shown in Fig.3.

.

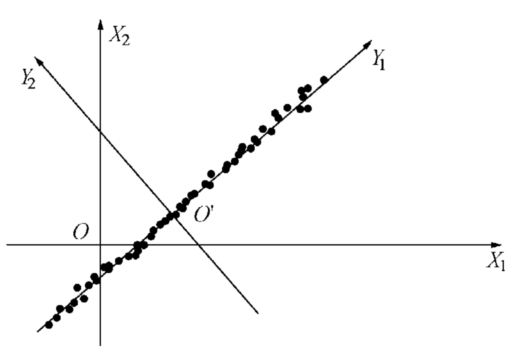

Fig. 3 Principal component analysis for two-dimensional vectors

It is easy that a linear combination can be constructed for the data of (x_1, x_2) shown in Fig.2.

$$\left.\begin{aligned} y_1 &= x_1\cos\theta + x_2\sin\theta + \beta_1, \\ y_2 &= -x_1\sin\theta + x_2\cos\theta + \beta_2\circ \end{aligned}\right\} \quad (2)$$

Some methods can be utilized to determine θ and β in the condition of variance of y_1, Var(y_1), achieving maximum. Hereby, the new vector of y_1 can basically display the distribution characters of (x_1, x_2). Therefore, some two-dimensional matrix can be approximately transferred into one-dimensional matrix. If the overall information needed, y_2, which can exhibit the vertical distribution characters, can be built. Here, y_1 and y_2 are respectively called the first and the second principal component of the two-dimensional matrix. Similarly, principal components for ploy-dimensional vector can also be constructed. The data for micro-structure of clay in this paper is a six-dimensional vector. The physical meaning of every vector is very different from others. Therefore, the first step is to obtain the standardization parameters of every vector. That is

$$x_i^* = \frac{x_i - \mu_i}{\sigma_i} \quad (i=1,2,\cdots,6) \qquad (3)$$

Here, μ_i and σ_i is average value and variance of variable x_i. Therefore, formula (1) can be transformed into formula (4).

$$x^* = \left(x_1^*,\ x_2^*,\ x_3^*,\ x_4^*,\ x_5^*,\ x_6^*\right)^{\mathrm{T}} \qquad (4)$$

From formula (4), a linear combination can be obtained like this:

$$y_1^* = a_{11}x_1^* + a_{12}x_2^* + a_{13}x_3^* + a_{14}x_4^* + a_{15}x_5^* + a_{16}x_6^* \qquad (5)$$

From the regulation of coordinate conversion, formula (6) is necessary.

$$a_1^{\mathrm{T}}a_1 = 1 \qquad (6)$$

Where, a_1 is the vector of (a_{11}, a_{12}, a_{13}, a_{14}, a_{15}, a_{16}). In formula (5), there are six undetermined coefficients need to be defined. When letting differential coefficient of y_1^* about x_1^* equals to zero in the condition of formula (6), a_{11} can be defined. Similarly, other coefficients in formula (5) can also be determined one by one. In addition, the maximum of $\mathrm{Var}\left(y_1^*\right)$ and y_1^* can be easily gained subsequently. It is generally speaking that y_1^* is the formula for the first principal component of formula (1). The second principal component can be constructed if the first one is not enough to illustrate necessary information of the original data. Namely

$$y_2^* = a_{21}x_1^* + a_{22}x_2^* + a_{23}x_3^* + a_{24}x_4^* + a_{25}x_5^* + a_{26}x_6^* \qquad (7)$$

In the process of determination of a_2= (a_{21}, a_{22}, a_{23}, a_{24}, a_{25}, a_{26})$^{\mathrm{T}}$, $\boldsymbol{y}_1^*$ and $\boldsymbol{y}_2^*$ should be considered uncorrelated independent random variable. That is

$$\mathrm{Cov}\left(y_2^*,\ y_1^*\right) = \mathrm{Cov}\left(a_2^{\mathrm{T}}x^*,\ a_1^{\mathrm{T}}x^*\right) = a_2^{\mathrm{T}}\sum a_1 = 0 \qquad (8)$$

Here, $\sum$ is the covariance matrix of vector x^*. Same to formula (6), formula (9) is the restricted condition in a_2 determination. Thereby,

$$a_2^{\mathrm{T}}a_2 = 1 \qquad (9)$$

Here, a_2 is the vector of (a_{21}, a_{22}, a_{23}, a_{24}, a_{25}, a_{26}). In the conditions of formula (8) and (9), a_2 can be determined as the differential coefficient of y_2^* about x_2^* equal zero. Consequently, the second principal component of formula (1) can be found. It is easy to achieve the third, the fourth, the fifth and the sixth principal component in the same way. Therefore, the following three formulae can be derived.

$$y^* = a^{\mathrm{T}} x^* \quad (10)$$

$$y^* = \left(y_1^*,\ y_2^*,\ y_3^*,\ y_4^*,\ y_5^*,\ y_6^*\right)^{\mathrm{T}} \quad (11)$$

$$a = \left(a_1,\ a_2,\ a_3,\ a_4,\ a_5,\ a_6\right) \quad (12)$$

In fact, the process of principal component determination can be used to define process of the characteristic roots of $\sum$, λ_i and the corresponding orthogonal unit characteristic vectors. The covariance matrix of y^* can be written as

$$\mathrm{Cov}\left(\boldsymbol{y}^*\right) = a^{\mathrm{T}} \sum a = \mathrm{Diag}\left(\lambda_1, \lambda_2, \lambda_3, \lambda_4, \lambda_5, \lambda_6\right) \quad (13)$$

The total variance of every principal component is

$$\sum_{i=1}^{6} \mathrm{Var}\left(\boldsymbol{y}_i^*\right) = \sum_{i=1}^{6} \lambda_i \quad (14)$$

It can be said that the total variance of the standardized variables, $\sum_{i=1}^{6} \mathrm{Var}\left(x_i^*\right)$, can be broken down as the sum of the six data which respectively are variances of the uncorrelated variables. In order to explore importance of the first principal component, the following variable can be defined.

$$\eta_1 = \frac{\lambda_1}{\sum_{i=1}^{6} \lambda_i} \quad (15)$$

The variable of η_1, called the contributing ratio of the first principal component, implies the rate of information carried by the principal component to that carried by the original matrix, formula (1). Similarly, the contributing ratio of the No. k principal component can be defined as η_k. Therefore, the cumulated contributing ratio of the former m principal components should be written as

$$\xi_m = \sum_{i=1}^{m} \eta_i \quad (16)$$

V. Pedigree Cluster Analysis for Micro-Structure

In this section, $l_{ij} = d(a_i,\ a_j)$ is defined as the distance between the element a_i and a_j. Namely

$$l_{ij} = \sqrt{\sum_{k=1}^{6} \left(\boldsymbol{a}_{ki} - \boldsymbol{a}_{kj}\right)^2} \quad (17)$$

If G_p and G_q are two different clusters constituted of n_p and n_q elements respectively, the centroids of G_p, $\bar{\boldsymbol{a}}_p$, and the centroids of G_q, $\bar{\boldsymbol{a}}_q$, can be written as

$$\bar{\boldsymbol{a}}_p = \frac{1}{n_p} \sum_{i=1}^{n_p} \boldsymbol{a}_i^{(p)} \quad (18a)$$

$$\bar{\boldsymbol{a}}_q = \frac{1}{n_q} \sum_{i=1}^{n_q} \boldsymbol{a}_i^{(q)} \quad (18b)$$

Here, $\boldsymbol{a}_1^{(p)}$, $\boldsymbol{a}_2^{(p)}$, …, $\boldsymbol{a}_{n_p}^{(p)}$ and $\boldsymbol{a}_1^{(q)}$, $\boldsymbol{a}_2^{(q)}$, …, $\boldsymbol{a}_{n_q}^{(q)}$ are the elements of the cluster G_p and cluster G_q.

4.1 Definition of distance between clusters

The most popular types of distance, used to evaluate characteristic of relationship between clusters, are the longest distance, the shortest distance, the average distance and the centroid distance.

(1) The longest distance defined as the longest distance between any two elements which respectively belongs to the two different clusters.

$$D_{pq} = \max_{i \in G_p, j \in G_q} d\left(\boldsymbol{a}_i, \boldsymbol{a}_j\right) \quad (19)$$

(2) The shortest distance defined as the shorted distance between any two elements which respectively belongs to the two different clusters.

$$D_{pq} = \min_{i \in G_p, j \in G_q} d\left(\boldsymbol{a}_i, \boldsymbol{a}_j\right) \quad (20)$$

(3) The average distance defined as the average distance between any two elements which respectively belongs to the two different clusters.

$$D_{pq} = \frac{1}{n_p n_q} \sum_{i \in G_p} \sum_{j \in G_q} d\left(\boldsymbol{a}_i, \boldsymbol{a}_j\right) \quad (21)$$

And (4) the centroid distance defined as the distance between the two clusters‘ centroids.

$$D_{pq} = d\left(\bar{\boldsymbol{a}}_p, \bar{\boldsymbol{a}}_q\right) \quad (22)$$

4.2 Deduction of distance between clusters

If the distance of cluster G_k to cluster G_p and cluster G_q is D_{pk} and D_{qk} respectively, cluster G_r is composed of G_p and G_q, the distance between cluster G_r and cluster G_k can be described as following.

(1) The longest distance

$$D_{rk} = \max\left\{D_{pk}, D_{qk}\right\} \quad (23)$$

(2) The shortest distance

$$D_{rk} = \min\left\{D_{pk}, D_{qk}\right\} \quad (24)$$

(3) The average distance

$$D_{rk} = \frac{n_p}{n_r} D_{pk} + \frac{n_q}{n_r} D_{qk} \quad (25)$$

And (4) the centroid distance

$$D_{rk} = \sqrt{\frac{n_p}{n_r} D_{pk}^2 + \frac{n_q}{n_r} D_{qk}^2 - \frac{n_p n_q}{n_r^2} D_{pq}^2} \quad (26)$$

4.3 The analysis process

The analysis process of pedigree cluster can be divided into several parts.

(1) Every SEM photos taken from the three different sections is solely set as a cluster at the beginning of analysis. 5 photos were taken in the horizontal section for every consolidated pressure. And that is to say there are 25 clusters (elements) at the beginning. The distance matrix $D_{(0)}$, which is a 25×25 phalanx, can be calculated from

formula (27) when the distances between any two clusters computed.

$$D_{(0)} = \begin{bmatrix} 0 & l_{1,2} & l_{1,3} & \cdots & l_{1,25} \\ l_{2,1} & 0 & l_{2,3} & \cdots & l_{2,25} \\ l_{3,1} & l_{3,2} & 0 & \cdots & l_{3,25} \\ \vdots & \vdots & \vdots & & \vdots \\ l_{25,1} & l_{25,2} & l_{25,3} & \cdots & 0 \end{bmatrix} \quad (27)$$

(2) The minimum in matrix $D_{(0)}$, $\min l_{pq}$, is selected and the corresponding cluster of G_p and G_q are combined into a new cluster G_r. The rows and the columns depended on G_p and G_q are eliminated from the matrix. At the same time, a new row and a new column, depended on the cluster G_r, are added into the matrix. Therefore, a new 24×24 matrix, $D_{(1)}$, is obtained.

(3) The process stated above is repeated, another new 23×23 matrix $D_{(2)}$, displayed the distance of clusters, can also be obtained. The process is repeated again and again until all clusters merged into one. Then the analysis process terminate.

And (4), based on the order number and analysis process, the scheme of pedigree cluster can be drawn.

VI. Comparison of Synthetical Parameters

The principal component indexes

The correlation coefficients between parameters of particles and pore aggregates for section *A* are list in table 2. It is clear that different parameter is correlative in some extent, especially a_2, a_3 and a_4.

Table 2 Correlation Coefficient Of Micro-Structure Parameters For Grain Aggregate And Pore Aggregate For Section *A*

Parameters		a_1	a_2	a_3	a_4	a_5	a_6
Particles	a_1	1	0.12	0.16	0.04	-0.61	0.78
	a_2		1	0.98	0.99	0.54	-0.27
	a_3			1	0.99	0.49	-0.23
	a_4		Symmetry		1	0.60	-0.33
	a_5					1	-0.64
	a_6						1
Pore	a_1	1	-0.06	-0.09	-0.17	-0.71	-0.06
	a_2		1	0.98	0.99	0.60	-0.13
	a_3			1	0.99	0.61	-0.13
	a_4		Symmetry		1	0.69	-0.13
	a_5					1	0.03
	a_6						1

Both for grain aggregate and for pore aggregate, correlations between a_2 and a_3, a_2 and a_4, a_3 and a_4 are all remarkable. That is to say some information displayed by the three parameters is reduplicate. Therefore, the reasonable method is to find some synthetical parameters, which are incorrelate to each other, to illustrate feature of SEM photos.

Table 3 Comparison Of Grain Principal Component To Pore's For The Five Group Samples

	Item	Ratio	Cumulated contributing ratio
For particles	The first principal component	0.596	0.596
	The second principal component	0.336	0.932
	The third principal component	0.051	0.983
For pores	The first principal component	0.593	0.593
	The second principal component	0.229	0.822
	The third principal component	0.156	0.977

It can be seen from the table 3 that the cumulated contributing ratio of the first and the second principal component for the particles and for the pores are 0.932 and 0.822 respectively. Therefore, it can be concluded that when the first two principal components are selected to illustrate properties of the SEM photo, the particle micro-structure is superior to the pore micro-structure.

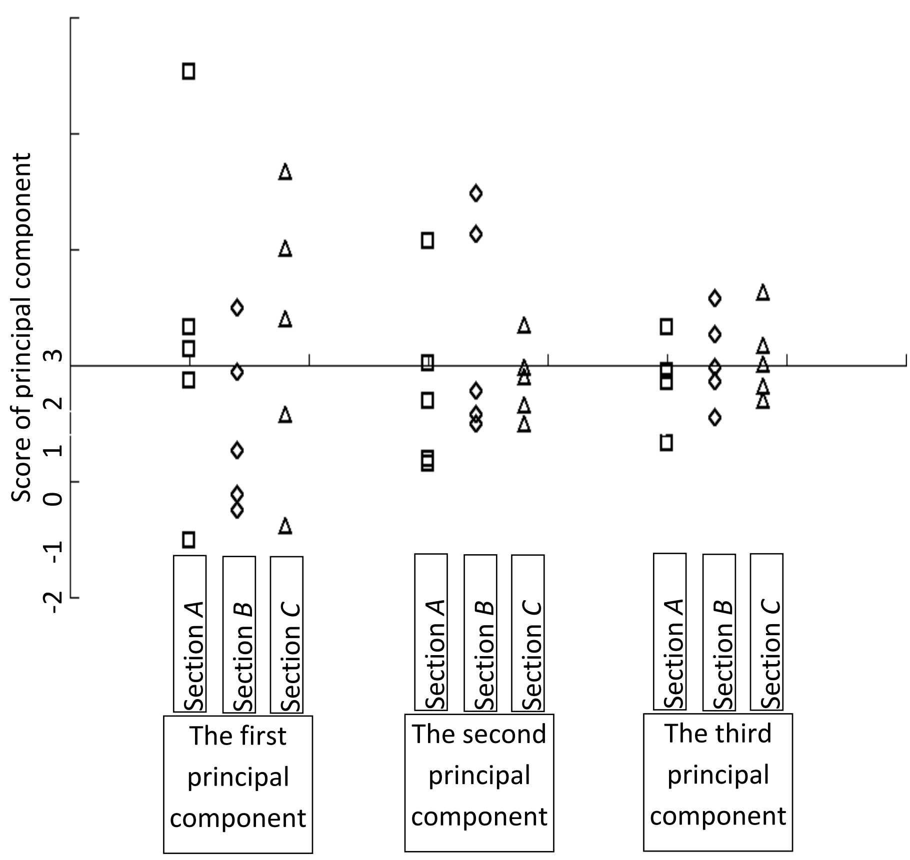

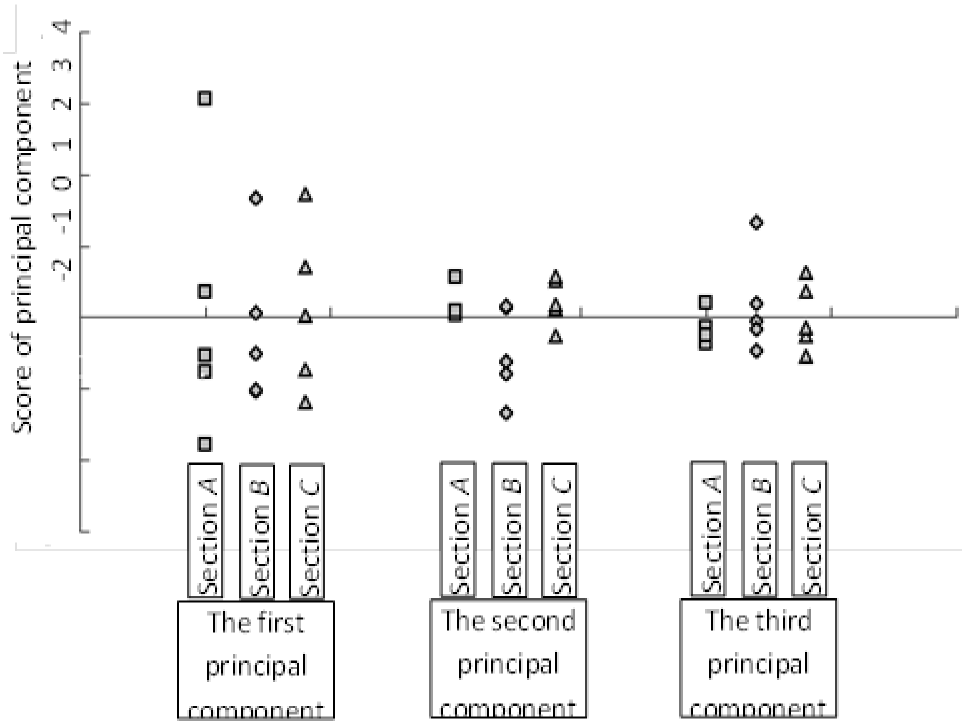

(b) Pore aggregate

Fig.4 Scores of the three principal components of the 5 groups

In the conditions of different consolidated pressure, scores of principal component for different sections are illustrated in Fig.4 carefully. The study on the SEM photos on section *A* is more meaning, interesting and instructive than that on other sections due to close and clear correlation between micro-structure of the three sections. Accordingly, the latter study is focused on the SEM photos from the section *A*.

For the SEM photos taken on the section *A*, the relationship of first three principal components with the consolidation pressure is shown in Fig.5. It is clear that the first principal component increases with the enlargement of the pressure, while the tendencies of the other two principal components are not very evident.

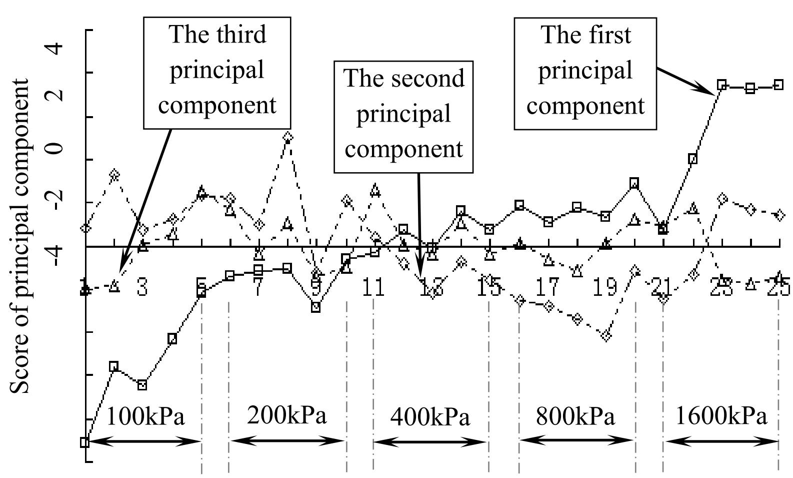

Fig.5 Scores of the three principal components of the 5 groups

The average of the first three principal components in the different consolidated are plot in Fig.6. At the same time, contributing ratio of the three principal components can be computed as 0.682、0.220 and 0.076 respectively. That is to say, the cumulated contributing ratio is 0.682, 0.902 and 0.979 correspondingly. It can be concluded that the first two (or the first three) principal components could display about 90.2% (or 97.9%) information displayed by the 6 original micro-structure parameters. Then, the original 6 dimensional parameters can be dimensionality reduced into 2 (or 3) accordingly.

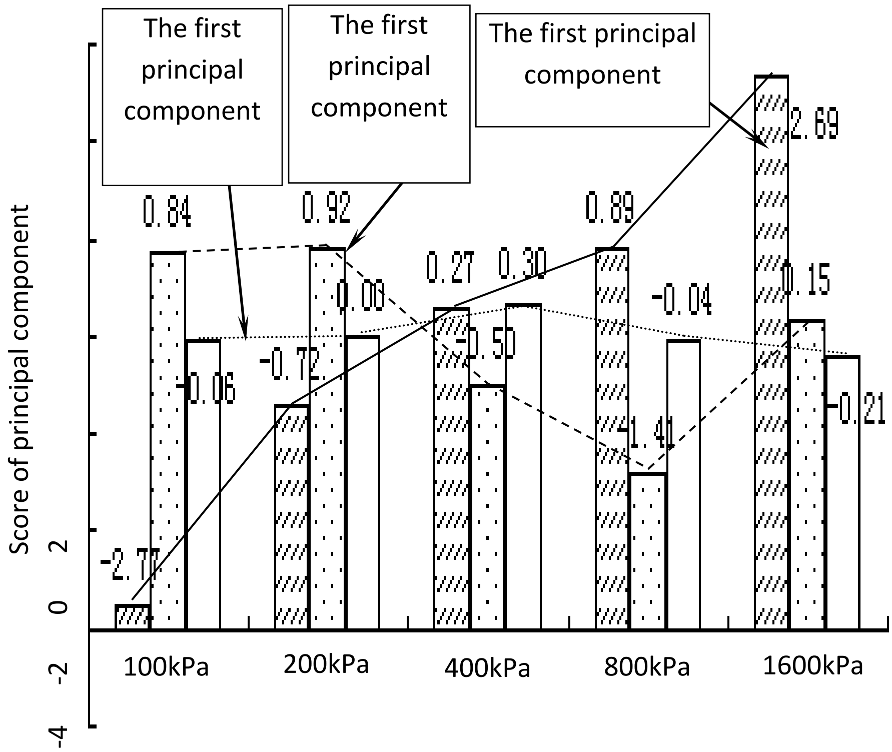

Fig.6 Means of the three principal components of the 5 groups

It is obvious from Fig.6 that the score of the first principal component climbs up from -2.77 to 2.69 with the increase of consolidated pressure from 100kPa to 1600kPa. Amplitude of variation for the first, the second and the third principal component is smaller and smaller. Other more, the second and the third principal component are all not monotone variables, while the first one is. Therefore, it is reasonable and necessary to introduce the first (or the first and the second) principal component into shear strength expressions and constitutive equations in order to reflect the micro-structure of the soil.

The linear fitting equation for the first principal component can be written as

$$m_1 = 0.003p - 1.795 \quad (28)$$

The corresponding correlation coefficient for linear fitting is R^2=0.83. The logarithmic fitting equation can be written as

$$m_1 = 1.81\ln p - 10.76 \quad (29)$$

The corresponding correlation coefficient is R^2=0.97. Here, m_1 is the first principal component and p is consolidated pressure.

Distance in cluster method

When average distance is used as the criterion in cluster method, the SEM photos on section *A* can be sorted as shown in Fig.7. It is distinct that all specimens are divided into 5 clusters depended on the five level different consolidated pressures. That is cluster *A*, *B*, *C*, *D* and *E* are corresponding to 1600Kpa, 800Kpa, 400Kpa, 200Kpa and 100Kpa, respectively. Thereby, taxonomic character of the micro-structure of soil in different consolidated pressure is remarkable. Subsequently, the cluster *A* and the cluster *B* are merged into a bigger cluster. The cluster *C* and the cluster *D* are merged into another bigger cluster, and then further combined with cluster *E* into a cluster. Therefore, it can be concluded that the specimens consolidated under the higher pressure conditions (>800kPa) are very different from those consolidated under lower pressure conditions.

\

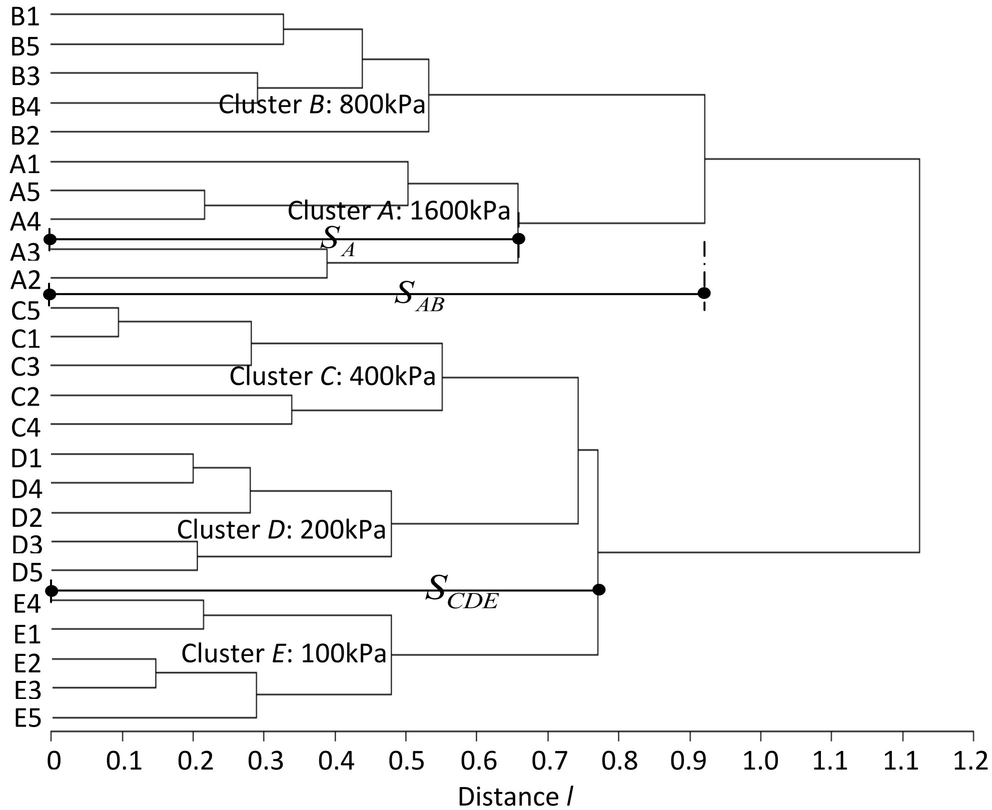

Fig.7 Result of the pedigree cluster of average distance method for different consolidation pressure

The concept of inner distance is defined as the distance between the small latest clusters in the new cluster. For example, the cluster *AB* is composed of the cluster *A* and the cluster *B*. Therefore, the inner distance of the cluster *AB* is the distance between the cluster *A* and *B*. Accordingly, the inner distance of the five cluster can be written as S_A, S_B, S_C, S_D and S_E. It is evident that S_A is the biggest one and S_D, S_E is the smallest one. The phenomenon may imply that the micro-structure properties of the soil consolidated under the higher pressure are more dispersive than that consolidated under the lower pressure.

VII. Conclusion

In this paper, two methods to evaluate characters of soil micro-structure are proposed and constructed and were successfully utilized to quantity the difference of the specimens obtained in consolidated condition. The first method is the principal component analysis and the second one is the cluster analysis. The studied specimens were cut from samples which had been consolidated in different five grades pressure. The study shows that the first principal component approximately linear increases with consolidation pressure. Consolidated specimens can be easily clustered into five families according to different consolidation pressure. Therefore, it is likely that synthetical parameters are superior to simple parameters in building constitutive equations in soil mechanics because the former can display the overall meaning of the micro-structure characteristic.

VIII. Acknowledgements

The work presented in this paper is part of the Study on *Determination of Shear Strength Indexes for Remolded Unsaturated Soil with Synthetic Micro-structure Parameters Taken into Consideration* (No. 200902276) research works funded by the China postdoctor science foundation and *A Method to Determine Shear Strength Indexes of frozen clay with micro-structure theory employed* (No. SKLFSE200906) funded by the State Key Laboratory of Frozen Soil Engineering in China. The authors would like to acknowledge Prof. Gang Zheng of the Tianjin University in China and Prof. Stefano Aversa of University of Naples Parthenope in Italy for the helpful suggestions and instruction.

IX. Reference

1) Hu R. L., Yeung M. R., Lee C. F., *et al*, 2001. Mechanical behavior and microstructural variation of loess under dynamic compaction. *Engineering Geology*, 59(3–4): 203-217.
2) Tippkötter, Rolf; Eickhorst, Thilo; Taubner, Heidi; et al, (2009). Detection of soil water in macropores of undisturbed soil using microfocus X-ray tube computerized tomography (μCT). *Soil and Tillage Research*, 105(1): 12-20.
3) Microstructure of saturated bentonites characterized by X-ray CT observations. Kawaragi, Chie; Yoneda, Tetsuro; Sato, Tsutomu; et al. *Engineering Geology*, 106(1-2): 51-57.

4) SHI Bin, JIANG Hong-tao, 2001. Research on the analysis techniques for clayey soil microstructure. *Chinese Journal of Rock Mechanics and Engineering*, 20(6): 864-870.
5) Schäffer, B.; Mueller, T.L.; Stauber, M.; et al. (2008). Soil and macro-pores under uniaxial compression. II. Morphometric analysis of macro-pore stability in undisturbed and repacked soil. *Geoderma*, 146(1-2): 175-182.
6) Schäffer, B.; Stauber, M.; Mueller, T.L.; et al 2008. Soil and macro-pores under uniaxial compression. I. Mechanical stability of repacked soil and deformation of different types of macro-pores. *Geoderma*, 146(1-2): 183-191.
7) Chertkov, V.Y. 2008. The physical effects of an intra-aggregate structure on soil shrinkage. *Geoderma*, 146(1-2): 147-156.
8) Agus, S. S. and Schanz, T., 2005. Effect of shrinking and swelling on microstructures and fabric of a compacted bentonite-sand mixture, *Proc. Int. Conf. on Problematic Soils, Cyprus,* 2, 543-550.
9) Bai, X. and Smart, P., 1997. Change in microstructure of kaolin in consolidation and undrained shear, *Géotechnique*, 47(5): 1009-1017.
10) Cui, Y. J., Loiseau, C., Delage, P., 2002. Microstructure change of a confined swelling soil due to suction controlled hydration, *Proc. 3rd Int. Conf. on Unsaturated Soils,* UNSAT' 2002, Recife, Brazil, Balkema, 2, 593-598.
11) Delage, P., Marcial, D., Cui, Y. J., et al. 2006. Ageing effects in a compacted bentonite: a microstructure approach. *Géotechnique*, 56 (5): 291-304.
12) Djéran-Maigre, I., Tessier, D., Grunberger, D., et al. 1998. Evolution of microstructures and of macroscopic properties of some clays during experimental compaction. *Marine and Petroleum Geology,* 15(2): 109-128.
13) Dudoignon, P., Pantet, A., Carrara, L. and Velde, B., 2001. Macro-micro measurement of particle arrangement in sheared kaolinitic matrices, *Géotechnique*, 51 (6): 493-499.
14) Tanaka, H. and Locat, J., 1999. A microstructural investigation of Osaka Bay clay: the impact of microfossils on its mechanical behavior, *Can. Geotech. J.,* 36(3):493-508.